arXiv:0809.2557v1 [astro-ph] 15 Sep 2008

A linear filter to reconstruct the ISW effect from CMB and LSS observations

R. B. Barreiro, P. Vielva, C. Hernández-Monteagudo and E. Martínez-González

***Abstract*—The extraction of a signal from some observational data sets that contain different contaminant emissions, often at a greater level than the signal itself, is a common problem in Astrophysics and Cosmology. The signal can be recovered, for instance, using a simple Wiener filter. However, in certain cases, additional information may also be available, such as a second observation which correlates to a certain level with the sought signal. In order to improve the quality of the reconstruction, it would be useful to include as well this additional information. Under these circumstances, we have constructed a linear filter, the linear covariance-based filter, that extracts the signal from the data but takes also into account the correlation with the second observation. To illustrate the performance of the method, we present a simple application to reconstruct the so-called Integrated Sachs-Wolfe effect from simulated observations of the Cosmic Microwave Background and of catalogues of galaxies.**

I. Introduction

THE issues of signal reconstruction and component separation have become of major importance in the field of Astrophysics and Cosmology, covering a large range of applications. In particular, Cosmic Microwave Background (CMB) observations require the development of sophisticated image processing techniques, in most cases on the sphere, to extract all the valuable information encoded in this type of data. The CMB is a relic radiation that was emitted shortly after the Big Bang, when the universe was $\sim$ 380000 years old and has travelled since then – almost unhindered – towards us, carrying a wealth of information about the origin and evolution of the universe (see e.g. [1], [2] and references therein). From the standard theory of inflation, the statistical distribution of the CMB anisotropies is expected to follow an isotropic and Gaussian random field on the sphere. Different physical phenomena leave their imprint in the CMB radiation that we observe today. In particular, a relevant contribution is given by the so-called Integrated Sachs-Wolfe (ISW) effect [3], which is due to the evolution in time of the gravitational potential, in the linear regime, of the Large Scale Structure (LSS) and its interaction with the CMB. This effect is of great interest since it provides a direct indication of either the presence of dark energy in the case of a flat universe or the existence of spatial curvature [4].

Using only CMB observations, it is difficult to obtain a direct detection of the ISW signal, since its contribution to the total CMB signal is, in general, small, and is difficult to disentangle it from other physical effects that also constitute the observed CMB picture. However, given the origin of this effect, a spatial correlation between the ISW and the LSS is expected. Therefore, it was suggested [5] that the signal of the ISW effect could be statistically detected by looking for cross-correlations between CMB and LSS observations. Following these ideas, different groups have obtained a statistical detection of the ISW effect using the CMB data provided by the WMAP NASA satellite and different LSS surveys at levels between 2.5σ and 4.5σ [6]–[16].

Nonetheless, it would be desirable to obtain not only a statistical detection of the ISW signal but also the actual map of this effect. A possible procedure would be to apply a reconstruction image technique (e.g. Wiener filter [17], maximum-entropy method [18]) to the CMB map in order to extract the ISW effect from the rest of contributions of the primordial radiation. However, given the weak level of the signal such a simple procedure is not expected to provide good results. Also, techniques that make use of multifrequency observations (see [19] and references therein) are not useful since the signal has the same frequency dependence as the other dominant CMB contributions. Thus, instead, we propose to recover the ISW map applying a filter, that we have called linear covariance-based (LCB) filter, to the CMB data that takes also into account the information coming from the cross-correlation between the CMB and the LSS surveys.

The outline of the paper is as follows. Section II presents our method to reconstruct a signal embedded in a noisy background and correlated with a second observation. Section III shows the performance of the proposed LCB filter in a simple application, the recovery of the ISW signal from simulated data sets. The robustness of the methodology against certain non-idealities is studied in section IV. Finally, we present our conclusions in section V.

II. The method

A random signal a measured on the sphere, such as the CMB, is usually expanded in terms of the spherical harmonics $Y_{\ell m}$

$$a(\theta,\phi) = \sum_{l=0}^{\infty}\sum_{m=-\ell}^{\ell} a_{\ell m} Y_{\ell m}(\theta,\phi) \qquad (1)$$

where $\theta \in [0,\pi]$ and $\phi \in [0,2\pi]$ stand for the colatitude and longitude in spherical coordinates, respectively, and $a_{\ell m}$ are the coefficients of the expansion. For a statistically isotropic signal, the variance of the coefficients is independent of m:

$$\langle a_{\ell m} a^*_{\ell' m'} \rangle = C_\ell \delta_{\ell\ell'} \delta_{mm'} \qquad (2)$$

R.B. Barreiro, P. Vielva and E. Martínez-González are at the Instituto de Física de Cantabria (CSIC-Universidad de Cantabria), Santander, Spain

Carlos Hernández-Monteagudo is at Max Planck Institut für Astrophysik, Munich, Germany

Manuscript received –; revised –.

where the averages are to be taken over statistical ensembles and the C_ℓ's constitute the angular power spectrum. For the case of an isotropic Gaussian random field on the sphere, the power spectrum completely characterises the signal.

A. Wiener filter (WF)

Let us assume that we have an observation d that contains a certain signal of interest s plus some generic noise n, both of which are assumed to be Gaussian and isotropic. One possible way to obtain an estimation $\hat{s}$ of the signal is to apply the classical WF to the data, which, at each (ℓ, m) mode, is given by:

$$\hat{s}_{\ell m} = \frac{C_\ell^s}{C_\ell^s + C_\ell^n} d_{\ell m} \tag{3}$$

where C_ℓ^s and C_ℓ^n correspond to the power spectrum of signal and noise respectively. It can be shown that WF is the linear filter that minimises the variance of the reconstruction error.

It is well known that the power spectrum of the WF reconstruction is biased towards values lower than the true signal, with the bias depending on the signal-to-noise ratio of the data. In particular, from the previous equation, it is straightforward to show that the expected value of the power spectrum for the reconstructed signal is given by

$$\left\langle C_\ell^{\hat{s}} \right\rangle = \frac{(C_\ell^s)^2}{C_\ell^s + C_\ell^n} \tag{4}$$

or, alternatively, we can write the expected bias of the signal as

$$\langle b \rangle = C_\ell^s - \left\langle C_\ell^{\hat{s}} \right\rangle = \frac{C_\ell^s C_\ell^n}{C_\ell^s + C_\ell^n} \tag{5}$$

Note that in the limit of infinite signal-to-noise ratio, the WF goes to unity and the bias becomes negligible.

B. Linear covariance-based (LCB) filter

Let us assume that we have an additional second observation g which is also isotropic and Gaussian and that is correlated with the signal s. It would be desirable to include the information of g in order to reconstruct s. The signals are characterised by their angular power spectra and also by their cross power spectrum:

$$C_\ell^{gs} = \langle g_{\ell m} s^*_{\ell' m'} \rangle \tag{6}$$

which we assume to be (statistically) known[1]. The covariance matrix $C(\ell)$ of g and s at each multipole ℓ is constituted by the expected power spectra of the signals (diagonal elements) and their cross-power spectrum (off-diagonal elements). It is useful to calculate the Cholesky decomposition of the covariance matrix, which satisfies $C(\ell) = L(\ell) L^T(\ell)$, where L is a lower triangular matrix. It can be shown that $g_{\ell m}$ and $s_{\ell m}$ can be written as

$$\begin{pmatrix} g_{\ell m} \\ s_{\ell m} \end{pmatrix} = \begin{pmatrix} L_{11}(\ell) & 0 \\ L_{12}(\ell) & L_{22}(\ell) \end{pmatrix} \begin{pmatrix} h_{\ell m} \\ j_{\ell m} \end{pmatrix} \tag{7}$$

[1]In the particular case of the ISW recovery, this corresponds to the expected cross-correlation between the ISW signal and the projected galaxy density. This quantity is given in terms of cosmological parameters that define the expansion and the energy content of the Universe, and the astrophysical laws that guide the LSS evolution.

where h and j are uncorrelated Gaussian variables of unit variance, sometimes referred to as hidden variables. Note that the elements of $L(\ell)$ relate to the elements of the covariance matrix $C(\ell)$ as $L_{11} = \sqrt{C_\ell^g}, L_{12} = C_\ell^{gs}/\sqrt{C_\ell^g}$ and $L_{22} = \sqrt{|C(\ell)|/C_\ell^g}$, where $|C(\ell)|$ is the determinant of the covariance matrix at each ℓ mode.

From the previous equation, we can trivially write s as a function of g and j as

$$s_{\ell m} = \frac{L_{12}(\ell)}{L_{11}(\ell)} g_{\ell m} + L_{22}(\ell) j_{\ell m} \tag{8}$$

Let us recall the observational data d, which can now be written as

$$d_{\ell m} = s_{\ell m} + n_{\ell m} = \frac{L_{12}(\ell)}{L_{11}(\ell)} g_{\ell m} + L_{22}(\ell) j_{\ell m} + n_{\ell m} \tag{9}$$

In order to recover s, we can now proceed in the following way. The first term of equation (8) can be easily calculated from g and the covariance matrix of the signals. The second term can be estimated by applying WF to the modified data $\bar{d}$ given by

$$\bar{d}_{\ell m} = d_{\ell m} - \frac{L_{12}(\ell)}{L_{11}(\ell)} g_{\ell m} = L_{22}(\ell) j_{\ell m} + n_{\ell m} \tag{10}$$

Therefore, the final estimation $\hat{s}$, at each multipole, is obtained as

$$\hat{s}_{\ell m} = \frac{L_{12}(\ell)}{L_{11}(\ell)} g_{\ell m} + \frac{L_{22}^2(\ell)}{L_{22}^2(\ell) + C_\ell^n} \bar{d}_{\ell m} \tag{11}$$

This simple procedure allows one to take into account the second correlated observation g in the reconstruction of s. This improves the quality of the reconstructed signal that also has the right correlation with g.

It can be easily shown that the expected value of the power spectrum for the reconstructed signal is given by

$$\left\langle C_\ell^{\hat{s}} \right\rangle = \frac{(C_\ell^{gs})^2 \left(|C(\ell)| + C_\ell^g C_\ell^n\right) + |C(\ell)|^2}{C_\ell^g \left(|C(\ell)| + C_\ell^g C_\ell^n\right)} \tag{12}$$

As we are using WF to recover a part of the signal, the power spectrum of the reconstruction is again biased. However, it can be shown that this bias is always lower or equal than the one of the WF reconstruction. To prove this statement, we first note that the cross power spectrum must satisfy $(C_\ell^{gs})^2 = \alpha C_\ell^g C_\ell^s$, with $0 \leq \alpha \leq 1$. Taking this property into account and making use of equation (12), we find that the bias introduced by the LCB filter is given by

$$\langle b \rangle = \frac{C_\ell^s C_\ell^n}{C_\ell^s + \frac{C_\ell^n}{1-\alpha}} \tag{13}$$

As one would expect, the bias is a function of C_ℓ^s, C_ℓ^n and α, but does not depend on C_ℓ^g. It is interesting to point out that for $\alpha = 0$, the LCB filter defaults to WF, since in this case g does not contain information about s. For $\alpha = 1$, the bias goes to zero, and the reconstructed signal is simply proportional to the observation g. Also, by comparing equations (5) and (13), and since $0 \leq \alpha \leq 1$, it becomes apparent that the bias of the LCB filter reconstruction is always lower or equal than the one of WF.

Finally, we would like to remark that the described procedure can be easily generalised to include additional correlated signals, providing the expected value of the full covariance matrix is known.

III. Reconstructing the ISW map

In order to test the performance of our method, we have considered the problem of reconstructing the ISW map from CMB and LSS observations. In our case, the signal s corresponds to the temperature fluctuations caused by the ISW effect, the observed data d is a CMB observation, the noise n is all the signal present in the CMB map that is not ISW and g is a catalogue of galaxies (i.e. a map of the galaxy density projected along the line of sight) which is correlated with the ISW pattern through the gravitational potential which affects to both. The reconstruction of the ISW map is a very challenging problem since the signal is very weak, in particular the signal-to-noise ratio for the considered example (maps with $\sim$ 2-degree resolution) is around 0.4. Although real CMB and LSS data are affected by non-idealities, like incomplete sky coverage and residual signals coming from astrophysical contaminants, in this section we will consider full-sky observations free of residual contaminants. The reason is that this simpler scenario allows one to understand better the performance of the LCB filter. However, in section IV we will study the robustness of the method in more realistic situations.

We have generated correlated simulations of CMB and catalogues of galaxies making use of equation (7) (see also [20]). More specifically, for a given model and at each multipole, first we calculate the covariance matrix $C(\ell)$ (using a modified version of CMBFAST [21]) and its corresponding Cholesky decomposition $L(\ell)$. Then, we generate two uncorrelated Gaussian variables, $h_{\ell m}$ and $j_{\ell m}$, of zero mean and unit dispersion. These quantities are then combined following equation (7) to obtain the coherent ISW and galaxy catalogue simulations. Finally, an independent Gaussian CMB simulation is generated (without including the ISW contribution) and added to the ISW map to obtain the simulated data d. Since the ISW effect is important at large angular scales, our simulated maps have a resolution of $\sim$ 2 degrees, corresponding to the HEALPix[2] parameter $n_{side} = 32$. For the CMB power spectra the flat Λ-CDM model that best fits the 3-year WMAP data [22] has been used. According to this model, the Universe has undergone a recent epoch of accelerated expansion, and the energy causing this acceleration amounts, at the present time, around 75 per cent of the total energy budget of the Universe. We have neither included a beam nor instrumental noise, since, for the current and future CMB observations, their effect is negligible at the considered angular scales. For the galaxy catalogue, we have generated several idealised surveys centred at different redshifts z (an astrophysical parameter related to the distance of the galaxies from the observer). It is known that galaxies are biased tracers of the underlying matter density field present in the Universe, in the sense that they tend to populate most of the times the most overdense regions of the Universe. This bias is dependent of the galaxy type, and a priori may depend as well on the age of the Universe (also related to the redshift parameter z). For simplicity we have considered a constant bias and a population of galaxies with no intrinsic evolution with redshift. It can be shown from equation (11) that the reconstruction of the signal is independent of a constant bias, since it acts as a global normalisation of the galaxy catalogue. The cross-power spectra between the CMB and the different catalogues of galaxies have been obtained following linear theory within the frame of the concordance ΛCDM cosmological model. This assumes that perturbations in the density field and gravitational potential are *small*, which is appropriate for the large scales relevant to the ISW effect (we know that the universe is isotropic and homogeneous in the very large scales). This computation traces the freeze-out of the growth of the gravitational potential wells due to the onset of an accelerated expansion in the Universe, and couples it to the gravitational energy that CMB photons gain or lose when crossing those potential wells.

As a measurement of the quality of the recovered signal, we will use the correlation coefficient ρ between the input and reconstructed maps which is defined as

$$\rho = \frac{\langle s\hat{s}\rangle - \langle s\rangle\langle\hat{s}\rangle}{\sigma_s\sigma_{\hat{s}}}, \tag{14}$$

where σ_s and $\sigma_{\hat{s}}$ are the dispersion of the input and reconstructed map respectively. Values of ρ closer to one provide better reconstructions. As an illustration, Fig. 1 shows a simulation of the ISW, the CMB (including the ISW) and a catalogue of galaxies centred at a comoving radial distance r corresponding to a redshift $z = 0.8$. The width of the radial shell containing the galaxies is roughly $0.1r$. Fig. 2 shows the reconstructed ISW map using the LCB filter (top panel) for the set of simulations given in Fig. 1. For comparison, the WF reconstruction is also shown (bottom panel). It is apparent that the map recovered with the LCB filter follows better the general structure of the input ISW map compared to that obtained with WF. This can also be seen from the cross-correlation coefficient between the input and reconstructed map which is 0.88 and 0.63 for the LCB and WF, respectively.

For a given CMB observation, the quality of the recovered ISW map obtained with the LCB filter could be significantly different depending on the catalogue of galaxies chosen for the reconstruction, since the cross-correlation between the ISW and the LSS is redshift dependent (as well as depends on the particular type of galaxies, the completeness of the survey, etc.). To provide an insight of the importance of this effect on the quality of the reconstruction, Fig. 3 shows the correlation coefficient (averaged over 1000 simulations) for the LCB filter using a CMB map and different LSS surveys, centred at redshift z (black solid thick line). We have also considered two widths in the range of redshifts observed by the survey: a wider bin centred on z (or on distance r) with a width of $0.1r$ (left panel) and a narrower bin of width $0.05r$ (right panel). The thinner solid curves provide the 1σ region around the mean ρ obtained from the simulations. For comparison, the results for the reconstruction from WF (red dashed thick line) and

[2]HEALPix is a hierarchical equal area isolatitude pixelization of the sphere. For more information see http://healpix.jpl.nasa.gov/

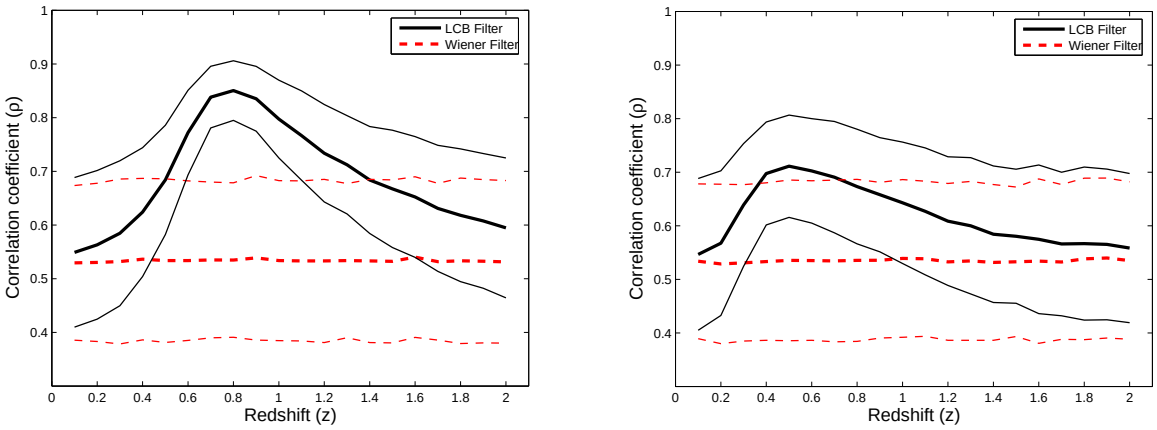

Fig. 3. Mean correlation coefficient for the ISW reconstruction using the LCB filter obtained from 1000 simulations (black solid thick line) and the corresponding 1σ region. Two cases are considered: a wider bin in z (left panel) and a narrower bin (right panel). For comparison the mean correlation coefficient and the corresponding 1σ region for the WF reconstruction are also shown (red dashed lines).

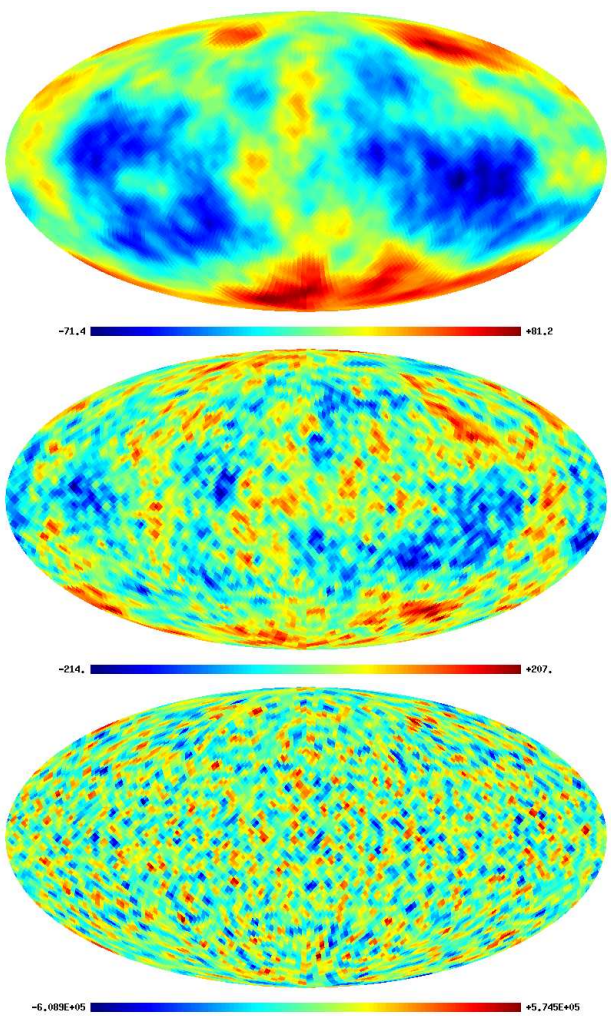

Fig. 1. The figure shows coherent simulations of an ISW map (top panel), a CMB map including the ISW effect (middle panel) and a catalogue of galaxies (bottom panel). The catalogue of galaxies has arbitrary units (the reconstruction is independent of the normalisation) and is centred at a comoving radial distance r corresponding to a redshift $z = 0.8$. The width of the radial shell containing the galaxies is approximately $0.1r$. The units of the CMB and ISW maps are microkelvin.

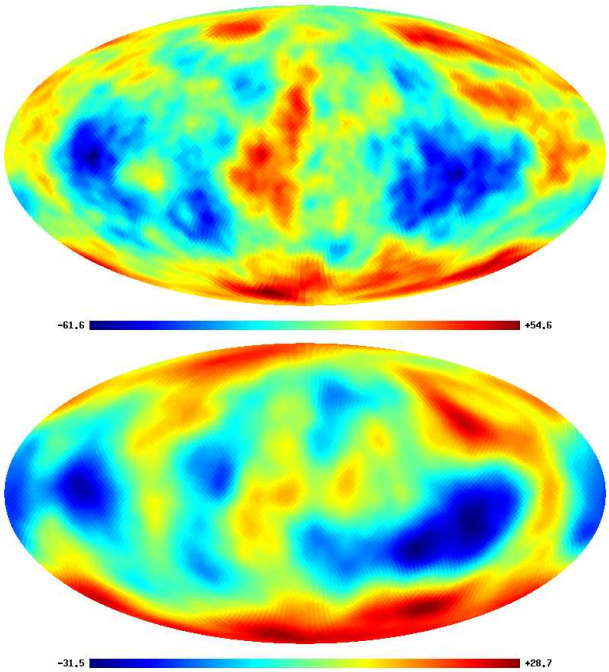

Fig. 2. Reconstruction of the ISW signal from the simulated data of Fig. 1 using the LCB filter (top) and the WF (bottom). The figures should be compared to the input ISW (top panel of Fig. 1). The cross-correlation coefficient ρ is equal to 0.88 and 0.63 for the LCB and WF reconstructions, respectively.

the corresponding 1σ region (red dashed thin lines) are also shown. Note that the WF reconstruction is independent of the considered LSS survey, since it does not use this information (the small deviations from a constant line are due to the finite number of simulations). From Fig. 3 it is apparent that the LCB filter outperforms the WF in all the considered cases. One can also notice that the surveys with a wider bin in z work better than those with a narrower bin. In particular, for the considered cases, we find that the best reconstruction is obtained for a survey centred in $z = 0.8$ for the case of the wider bin. This indicates that having a larger number of observed galaxies

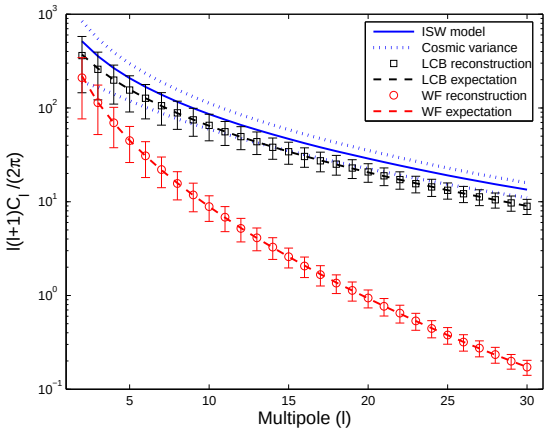

Fig. 4. Mean power spectrum of the ISW reconstruction using the LCB filter obtained from 1000 simulations (black squares) compared to the input model (blue solid line). The blue dotted lines indicate the 1σ region allowed by the cosmic variance and the error bars give the dispersion of the reconstructed power spectrum obtained from simulations. The theoretical expectation for the power spectrum of the reconstruction is also plotted (black dashed line). For comparison, the same quantities are given for the Wiener filter case (red circles and red dashed line). The reconstructions correspond to the wider bin case, centred at $z = 0.8$.

increases the correlation between the ISW and the considered survey and that, therefore, the reconstruction of the ISW signal is improved. However, we should remark that the bias between the galaxy and the underlying matter distribution is more unlikely to remain constant (as we have assumed) for wide bins. For this reason, a more detailed study of the bias within the redshift/distance bin would be required.

It is also interesting to point out that the quality of the reconstruction is higher in the hottest and coldest spots of the ISW map, since the signal is comparatively larger in those regions. For instance, for the best reconstruction case, the average correlation coefficient increases from $\rho = 0.85$, when all the pixels are considered, to $\rho = 0.94$, when only the pixels outside the 1σ region are considered.

We have also studied the power spectrum of the recovered ISW map, which provides an alternative measurement of the quality of the reconstruction. As mentioned in section II, we expect the power spectrum of our recovered ISW map to be biased at a certain level. Fig. 4 shows the power spectrum of the reconstructed ISW using the LCB filter averaged over 1000 simulations (black squares) for the case of a catalogue of galaxies covering a wide bin centred at redshift $z = 0.8$, compared to the input ISW model (blue solid line). The blue dotted lines correspond to the theoretical cosmic variance while the error bars give the dispersion obtained from simulations. For comparison, the expected reconstructed power spectrum given by equation (12) is also plotted (black dashed line), showing an excellent agreement with the results obtained from simulations. Although, as expected, the reconstructed power spectrum is biased, taking into account the weakness of the ISW effect, a significant part of the power of the signal is present in the reconstructed map. In particular, the average reconstructed power spectrum lies within the allowed 1σ cosmic variance region up to $\ell \sim 15$. We have also studied, for the same case, the average power spectrum and dispersion of the reconstructed ISW map using WF (red circles and error bars in Fig. 4), finding a much larger bias, in agreement with equation (4) (red dashed line). This shows again that combining information from the CMB and LSS, as in the LCB filter, is very useful to recover the ISW map.

IV. Robustness of the method

In the previous section, we have shown the performance of the LCB filter to recover the ISW effect from CMB and LSS observations in ideal conditions. However, when dealing with real data, they will be affected by different non-idealities, that should be taken into account in the analysis. Regarding CMB data, one of the most important issues is the contamination due to different astrophysical emissions, which is particularly strong in the Galactic plane. This region is usually discarded from the data, by applying a Galactic mask (i.e. replacing with zeroes the most contaminated regions). Regarding catalogues of galaxies, they do not usually cover the whole sky and, therefore, it is necessary to deal with incomplete sky maps.

In order to test the robustness of the LCB filter on an incomplete sky, we have repeated the analysis from the previous section after applying a simple mask to the data that covers around 25 per cent of the sky (see top panel of Fig. 5). The mask has been constructed as the addition of a band centred in the equator with latitude $|b| \leq 8°$ plus a circle centred in the southern ecliptic circle with a radius of 40°. The equatorial band mimics a simple Galactic mask from a CMB observation, discarding ~ 15 per cent of the sky, which is similar, for instance, to the area covered by the WMAP Kp2 mask [23]. The circle mimics a region not observed by an incomplete galaxy survey, as in the case of the NVSS catalogue [24].

The top panel of Fig. 5 shows the reconstruction of the ISW map using the LCB filter from the simulated data of Fig. 1 after applying the considered mask. The cross-correlation coefficient ρ, obtained outside the masked region, is 0.81 to be compared to ρ=0.88 in the ideal case. A more detailed study of the effect of the mask on the quality of the reconstruction is given in the left panel of Fig. 6, where the mean and dispersion of the correlation coefficient for the ISW reconstruction is shown for the LCB filter (black solid lines) and for the WF (red dashed lines), considering the case of the wider bin in z. This should be compared to the results obtained for the same case assuming ideal conditions, given in the left panel of Fig. 3. We can see that the presence of the mask reduces, although only at the level of a few per cent, the correlation between the input and reconstructed maps. For instance, for the best reconstruction, corresponding to a catalogue of galaxies centred at $z = 0.8$, the mean value of the correlation coefficient is reduced from 0.85, in the ideal case, to 0.81, when the mask is present. Therefore, the performance of the LCB filter is robust against incomplete sky observations. Regarding WF, the mean correlation coefficient is very similar to the one obtained in the ideal case.

Another interesting issue is the robustness of the method against uncertainties in the knowledge of the covariance matrix $C(\ell)$ or, for the considered case of the ISW reconstruction,

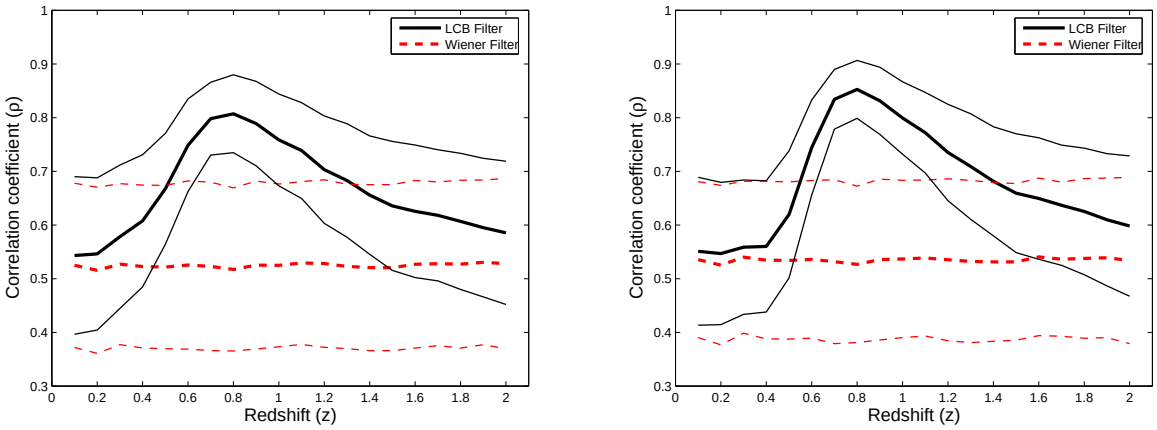

Fig. 6. Mean correlation coefficient for the ISW reconstruction using the LCB filter obtained from 1000 simulations (black solid thick line) and the corresponding 1σ region (black thin lines) for different galaxy surveys (considering the case of the wider bin in z). The left panel corresponds to reconstructions obtained from data where a mask is applied (discarding around one-fourth of the sky) and the right panel shows the results obtained assuming a *w*rong cosmological model. For comparison, the mean correlation coefficient and the corresponding 1σ region for the WF reconstruction are also shown (red dashed lines).

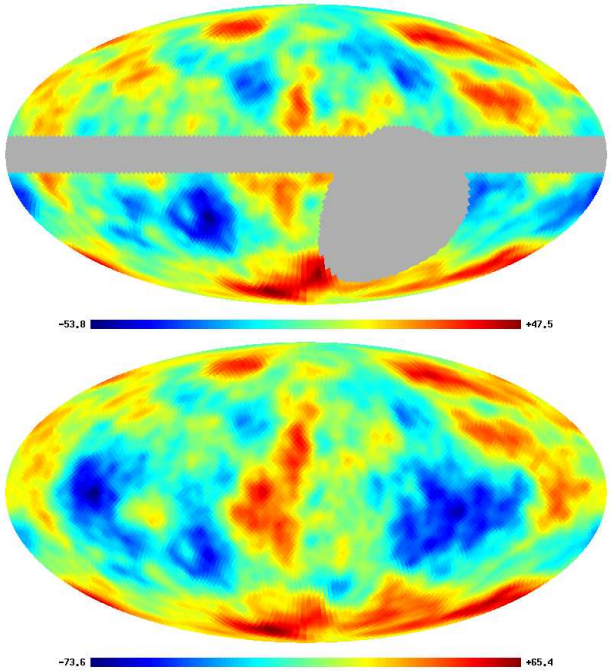

Fig. 5. Reconstruction of the ISW signal for the case of an incomplete sky (top) and when assuming an erroneous cosmological model (bottom). The figures should be compared to the input ISW (top panel of Fig. 1) and also to the reconstruction in the ideal case (top panel of Fig. 2). The grey region of the top panel indicates the masked region, excluded from the analysis. The cross-correlation coefficient ρ is equal to 0.81 (top reconstruction) and 0.87 (bottom reconstruction).

in the knowledge of the cosmological model. In the previous examples, we have used the same cosmological model to generate the simulations and to reconstruct the ISW map. However, in a more realistic case, the assumed cosmological parameters may deviate, at a certain level, from their true underlying values.

Different cosmological data sets (such as CMB, LSS galaxy surveys, primordial Big-Bang nucleosynthesis, measurements of the Hubble constant or supernovae data) are currently placing strong constraints on the cosmological parameters, giving rise to a consistent picture of the universe, the so-called concordance model. Therefore, given the current constraints, large deviations from the present estimation of the cosmological parameters are not expected. In order to test the sensitivity of the LCB filter to possible errors in the assumed cosmological model, we have produced reconstructions of the ISW map using a model different from the one present in the simulations (which was given by the Λ-CDM model that best fitted the 3-year WMAP data), i.e, we obtain the reconstructions using a *w*rong covariance matrix. This second model corresponds to the parameters given by the Λ-CDM model that best fits the 5-year WMAP data, baryon acoustic oscillations in the distribution of galaxies and Type I supernovae data (see [25] and references therein). The differences between these two models correspond to the level of uncertainties that one would expect in our present knowledge of the cosmological parameters. In particular, the value of the dark energy density Ω_Λ, one of the parameters more closely related to the ISW signal, differs in a ~ 5 per cent between both models.

The bottom panel of Fig. 5 shows the reconstruction of the ISW map using the LCB filter, assuming the alternative cosmological model, from the simulated data of Fig. 1. Although, in this case, the amplitude of the reconstructed ISW is a bit larger (due to the different assumed cosmological model), the correlation coefficient ($\rho = 0.87$) is still very similar to the value found in the ideal case. In addition, the right panel of Fig. 6 shows the mean and dispersion of the correlation coefficient for the ISW reconstruction in this case, averaged over a large number of simulations and considering the case of the wider bin in z. Again, the figure should be compared to the same case assuming ideal conditions, given in the left panel of Fig. 3. From the comparison, it is apparent that the assumption of a different cosmological model does not affect significantly the mean correlation coefficient between input and reconstructed ISW map neither for the LCB filter nor

for the WF. This result shows that our methodology is also robust against the possible uncertainties in our knowledge of the cosmological parameters.

V. Conclusions

We have presented a linear filter, the LCB filter, which reconstructs a signal from a confusion background taking into account additional information from a second observation correlated with the sought signal. To study the performance of the technique, we have applied it to simulated CMB and LSS observations with the aim of recovering the ISW effect. This is a very challenging problem, due to the weakness of the ISW signal and, as far as we know, this is the first time that a technique is presented that attempts to recover an ISW map instead of searching for a statistical detection of the signal. We have considered different possibilities for the LSS survey, in order to illustrate the dependence of the method on the characteristics of the chosen catalogue of galaxies. From the considered cases, the best reconstruction (mean $\rho = 0.85$) is obtained for a survey with a wide bin in z and centred in $z = 0.8$. For comparison, we have also recovered the ISW signal from CMB simulated maps using a classical WF, finding that the LCB filter provides better reconstructions. This confirms the idea that combining information from the CMB and the LSS survey is useful to recover the ISW map. We have also shown that our methodology is robust when dealing with incomplete sky observations and against the possible uncertainties in our knowledge of the cosmological model. In a future work we will present a more detailed application to the ISW effect that takes into account more realistic physical conditions for the galaxy populations. Finally, we would like to point out that the formalism can be easily generalised to include information from several galaxy surveys at the same time.

Acknowledgement

RBB, PV and EMG acknowledge partial financial support from the Spanish MEC project AYA2007-68058-C03-02. CHM acknowledges the hospitality of IFCA at Santander (Spain), where part of this work was carried out. Some of the results in this paper have been derived using the HEALPix [26] package.

References

[1] A. Challinor, "Cosmic Microwave Background Anisotropies," in *The Physics of the Early Universe*, ser. Lecture Notes in Physics, Berlin Springer Verlag, K. Tamvakis, Ed., vol. 653, 2005, pp. 71–+.

[2] E. Martínez-González and P. Vielva, "The Cosmic Microwave Background Anisotropies: Open Problems," in *The Many Scales in the Universe: JENAM 2004 Astrophysics Reviews*, J. C. Del Toro Iniesta, E. J. Alfaro, J. G. Gorgas, E. Salvador-Sole, and H. Butcher, Eds., Jan. 2006, pp. 1–4020.

[3] R. K. Sachs and A. M. Wolfe, "Perturbations of a Cosmological Model and Angular Variations of the Microwave Background," *The Astrophysical Journal*, vol. 147, pp. 73–+, Jan. 1967.

[4] P. J. Peebles and B. Ratra, "The cosmological constant and dark energy," *Reviews of Modern Physics*, vol. 75, pp. 559–606, Apr. 2003.

[5] R. G. Crittenden and N. Turok, "Looking for a Cosmological Constant with the Rees-Sciama Effect," *Physical Review Letters*, vol. 76, pp. 575–578, Jan. 1996.

[6] P. Fosalba, E. Gaztañaga, and F. J. Castander, "Detection of the Integrated Sachs-Wolfe and Sunyaev-Zeldovich Effects from the Cosmic Microwave Background-Galaxy Correlation," *The Astrophysical Journal Letters*, vol. 597, pp. L89–L92, Nov. 2003.

[7] S. Boughn and R. Crittenden, "A correlation between the cosmic microwave background and large-scale structure in the Universe," *Nature*, vol. 427, pp. 45–47, Jan. 2004.

[8] P. Fosalba and E. Gaztañaga, "Measurement of the gravitational potential evolution from the cross-correlation between WMAP and the APM Galaxy Survey," *Monthly Notices of the Royal Astronomical Society*, vol. 350, pp. L37–L41, May 2004.

[9] N. Afshordi, Y.-S. Loh, and M. A. Strauss, "Cross-correlation of the cosmic microwave background with the 2MASS galaxy survey: Signatures of dark energy, hot gas, and point sources," *Physical Review D*, vol. 69, no. 8, pp. 083 524–+, Apr. 2004.

[10] M. R. Nolta, E. L. Wright, L. Page, C. L. Bennett, M. Halpern, G. Hinshaw, N. Jarosik, A. Kogut, M. Limon, S. S. Meyer, D. N. Spergel, G. S. Tucker, and E. Wollack, "First Year Wilkinson Microwave Anisotropy Probe Observations: Dark Energy Induced Correlation with Radio Sources," *The Astrophysical Journal*, vol. 608, pp. 10–15, Jun. 2004.

[11] P. Vielva, E. Martínez-González, and M. Tucci, "Cross-correlation of the cosmic microwave background and radio galaxies in real, harmonic and wavelet spaces: detection of the integrated Sachs-Wolfe effect and dark energy constraints," *Monthly Notices of the Royal Astronomical Society*, vol. 365, pp. 891–901, Jan. 2006.

[12] D. Pietrobon, A. Balbi, and D. Marinucci, "Integrated Sachs-Wolfe effect from the cross correlation of WMAP 3year and the NRAO VLA sky survey data: New results and constraints on dark energy," *Physical Review D*, vol. 74, no. 4, pp. 043 524–+, Aug. 2006.

[13] J. D. McEwen, P. Vielva, M. P. Hobson, E. Martínez-González, and A. N. Lasenby, "Detection of the integrated Sachs-Wolfe effect and corresponding dark energy constraints made with directional spherical wavelets," *Monthly Notices of the Royal Astronomical Society*, vol. 376, pp. 1211–1226, Apr. 2007.

[14] J. D. McEwen, Y. Wiaux, M. P. Hobson, P. Vandergheynst, and A. N. Lasenby, "Probing dark energy with steerable wavelets through correlation of WMAP and NVSS local morphological measures," *Monthly Notices of the Royal Astronomical Society*, vol. 384, pp. 1289–1300, Mar. 2008.

[15] A. Raccanelli, A. Bonaldi, M. Negrello, S. Matarrese, G. Tormen, and G. de Zotti, "A reassessment of the evidence of the Integrated Sachs-Wolfe effect through the WMAP-NVSS correlation," *Monthly Notices of the Royal Astronomical Society*, vol. 386, pp. 2161–2166, Jun. 2008.

[16] T. Giannantonio, R. Scranton, R. G. Crittenden, R. C. Nichol, S. P. Boughn, A. D. Myers, and G. T. Richards, "Combined analysis of the integrated Sachs-Wolfe effect and cosmological implications," *ArXiv e-prints*, vol. 801, Jan. 2008.

[17] D. Wiener, *Extrapolation and Smoothing of Stationary Time Series*. New York, Wiley, 1949.

[18] J. Skilling, Ed., *Maximum entropy and bayesian methods : 8 : 1988*, 1989.

[19] J. Delabrouille and J.-F. Cardoso, "Diffuse source separation in CMB observations," *ArXiv Astrophysics e-prints*, Feb. 2007.

[20] S. P. Boughn, R. G. Crittenden, and N. G. Turok, "Correlations between the cosmic X-ray and microwave backgrounds: constraints on a cosmological constant," *New Astronomy*, vol. 3, pp. 275–291, Jul. 1998.

[21] U. Seljak and M. Zaldarriaga, "A Line-of-Sight Integration Approach to Cosmic Microwave Background Anisotropies," *The Astrophysical Journal*, vol. 469, pp. 437–+, Oct. 1996.

[22] D. N. Spergel, R. Bean, O. Doré, M. R. Nolta, C. L. Bennett, J. Dunkley, G. Hinshaw, N. Jarosik, E. Komatsu, L. Page, H. V. Peiris, L. Verde, M. Halpern, R. S. Hill, A. Kogut, M. Limon, S. S. Meyer, N. Odegard, G. S. Tucker, J. L. Weiland, E. Wollack, and E. L. Wright, "Three-Year Wilkinson Microwave Anisotropy Probe (WMAP) Observations: Implications for Cosmology," *The Astrophysical Journal Supplement Series*, vol. 170, pp. 377–408, Jun. 2007.

[23] C. L. Bennett, R. S. Hill, G. Hinshaw, M. R. Nolta, N. Odegard, L. Page, D. N. Spergel, J. L. Weiland, E. L. Wright, M. Halpern, N. Jarosik, A. Kogut, M. Limon, S. S. Meyer, G. S. Tucker, and E. Wollack, "First-Year Wilkinson Microwave Anisotropy Probe (WMAP) Observations: Foreground Emission," *The Astrophysical Journal Supplement Series*, vol. 148, pp. 97–117, Sep. 2003.

[24] J. J. Condon, W. D. Cotton, E. W. Greisen, Q. F. Yin, R. A. Perley, G. B. Taylor, and J. J. Broderick, "The NRAO VLA Sky Survey," *The Astronomical Journal*, vol. 115, pp. 1693–1716, May 1998.

[25] E. Komatsu, J. Dunkley, M. R. Nolta, C. L. Bennett, B. Gold, G. Hinshaw, N. Jarosik, D. Larson, M. Limon, L. Page, D. N. Spergel, M. Halpern, R. S. Hill, A. Kogut, S. S. Meyer, G. S. Tucker, J. L. Weiland, E. Wollack, and E. L. Wright, "Five-Year Wilkinson Microwave Anisotropy Probe (WMAP) Observations: Cosmological Interpretation," *ArXiv e-prints*, vol. 803, Mar. 2008.

[26] K. M. Górski, E. Hivon, A. J. Banday, B. D. Wandelt, F. K. Hansen, M. Reinecke, and M. Bartelmann, "HEALPix: A Framework for High-Resolution Discretization and Fast Analysis of Data Distributed on the Sphere," *The Astrophysical Journal*, vol. 622, pp. 759–771, Apr. 2005.

PLACE PHOTO HERE

R.B. Barreiro obtained her B.S. degree in 1995 from the Universidad de Santiago de Compostela, Spain, completing also as part of her degree one year at the University of Sheffield, UK. She completed her Ph.D. in astrophysics in the Universidad de Cantabria in 1999. After her Ph.D., she worked as a Research Associate at the Cavendish Laboratory of the University of Cambridge, UK. In 2002, she moved to the Instituto de Física de Cantabria (IFCA, CSIC-UC), Spain, with a long term contract. Currently, she continues at IFCA as a tenured scientist of the Universidad de Cantabria. Her research interests are mainly focused in the field of the cosmic microwave background, including statistical data analysis, in particular the study of the Gaussianity of the CMB, and the development of component separation techniques for both diffuse emissions and compact sources.

PLACE PHOTO HERE

P. Vielva is a *Ramón y Cajal* researcher of the Instituto de Física de Cantabria (IFCA, CSIC-UC). He obtained his B.S. degree in 1998 from the Universidad de Cantabria. He completed his Ph.D., at IFCA. In 2004 he was a postdoctoral researcher at the Collège de France/APC in Paris. In 2005 he moved to IFCA were he was a researcher of the Universidad de Cantabria associated to the ESA Planck mission. In 2006 he obtained an CSIC-I3P position at IFCA and during that year he was a visiting researcher at the Cavendish Laboratory of the University of Cambridge. His researching field is cosmology, specially the study of the cosmic microwave background (CMB). In particular, he works on the development and application of statistical and signal processing tools for the CMB data analysis.

PLACE PHOTO HERE

C. Hernández-Monteagudo is currently a post-doc at the Max Planck Institut für Astrophysik in Munich (Germany). He finished his Ph.D. in Physics at the University of Salamanca (Spain) in February 2002, and since then he has been doing research at the Max Planck Institut für Astrophysik in Munich and the University of Pennsylvania (USA). His interests span different aspects of the study of the Cosmic Microwave Background (CMB) radiation, such as cosmological recombination, reionization, pollution of the Inter Galactic Medium with the first metals, Comptonization of the CMB spectrum via the thermal Sunyaev-Zel'dovich effect, and other secondary effects such as kinetic Sunyaev-Zel'dovich effect, Rees Sciama and Integrated Sachs-Wolfe effect. Currently he is involved in three major projects in Cosmology: Planck (an ESA mission that attempts to measure CMB intensity and polarization anisotropies with unprecedented sensitivity and systematic control), the Atacama Cosmology Telescope (a collaboration in the US probing the small scales of the CMB angular power spectrum) and the PAU-BAU consolider project (a Spanish collaboration devoted to the study of the nature of Dark Energy).

PLACE PHOTO HERE

E. Martínez-González is currently a Research Professor at the Instituto de Física de Cantabria (IFCA, CSIC-UC). He obtained his B.S. degree in the Universidad de Cantabria in 1986 and followed his doctorate studies at NORDITA (Copenhagen, Denmark). He was the coordinator of the first European Research Network on the CMB funded by the EU. Currently, he is Co-Investigator of the Planck Low Frequency Instrument consortium. His research fields cover different theoretical and observational aspects of Cosmology, mainly focusing on the Cosmic Microwave Background.